Chapter 19
Structural Modal Identification Through High Speed Camera Video: Motion Magnification

Justin G. Chen, Neal Wadhwa, Young-Jin Cha, Frédo Durand, William T. Freeman, and Oral Buyukozturk

Abstract Video cameras offer the unique capability of collecting high density spatial data from a distant scene of interest. They could be employed as remote monitoring or inspection sensors because of their commonplace use, simplicity, and relatively low cost. The difficulty is in interpreting the video data into a usable format, such as displacement, that is familiar to engineers. A methodology called motion magnification, developed for visualizing exaggerated versions of small displacements, is extended to modal identification in structures. Experiments in a laboratory setting on a cantilever beam were performed to verify the method against accelerometer and laser vibrometer measurements. Motion magnification is used for modal analysis of cantilever beams to visualize mode shapes and calculate mode shape curvature as a basis for damage detection. Suggestions for applications of this methodology and challenges in real-world implementations are given.

Keywords Computer vision • Standoff condition assessment • Modal identification • Mode shape • High speed video

19.1 Introduction

Modal analysis of structures depends on the accurate and swift collection of data from a vibrating structure so the data can be later analyzed to determine the modal characteristics. The end goal for the development of a sensor system for modal analysis is to be able to robustly, precisely, quickly, and remotely collect data from a vibrating structure. Contact accelerometers are commonly used for modal analysis and are extremely accurate, however densely instrumenting a structure is difficult and tedious, and when the structure is small compared to the size of an accelerometer, the presence of added mass from accelerometers can affect the result. Non-contact methods of measurement avoid these draw backs and are being researched intensely for the purposes of modal analysis.

Non-contact methods of vibration measurement generally depend on some sort of electromagnetic radiation to transmit the information. Microwave interferometry has been studied [1], and laser methods such as laser vibrometry have also been studied [2]. Cameras measuring visible light provide an interesting method for measuring movement. They can range from precise instruments for high-frequency and high-resolution video or inexpensive units such as those on cell phones. There are also cameras that already monitor infrastructure for traffic or security reasons.

Motion can be quantified in video using a number of image processing techniques. Less sophisticated methods use edge detection, target objects, or lights to more easily measure any structural motion [3–5]. More recent methods make use of computer vision techniques, such as measurements of optical flow to determine the displacements of structures which is related to the techniques to be presented in this paper [6].

Recently, new computer vision techniques, collectively called motion magnification, were introduced to magnify small motions in videos [7–9]. The most recent motion magnification techniques use a signal processing approach to analyze image

J.G. Chen • Y.-J. Cha • O. Buyukozturk (✉)
Department of Civil and Environmental Engineering, Massachusetts Institute of Technology, 77 Massachusetts Avenue, Cambridge, MA 02139, USA
e-mail: obuyuk@mit.edu

N. Wadhwa • F. Durand • W.T. Freeman
Computer Science and Artificial Intelligence Laboratory, Massachusetts Institute of Technology, 77 Massachusetts Avenue, Cambridge, MA 02139, USA

J. De Clerck (ed.), *Topics in Modal Analysis I, Volume 7: Proceedings of the 32nd IMAC, A Conference and Exposition on Structural Dynamics, 2014*, Conference Proceedings of the Society for Experimental Mechanics Series,
DOI 10.1007/978-3-319-04753-9_19, © The Society for Experimental Mechanics, Inc. 2014

motions in a way analogous to an Eulerian framework for fluid flow analysis. They are ideal for computing and visualizing mode shapes because they are capable of detecting small subpixel motions that are present in the modal motions of vibrating structures and because they are able to separate the different modal motions through the use of temporal filtering.

The objective of this paper is to show how a camera can be used with computer vision techniques and motion magnification to identify the mode shapes of a cantilever column. We will first present the theory behind how videos can be analyzed for sensing of displacements or mode shapes. Then, results from a verification experiment comparing the derived displacements from a camera to a laser vibrometer and accelerometer measurement will be presented. Measurements identifying the mode shapes of a cantilever beam will be presented, and conclusions and suggestions for future studies will be given.

19.2 Derivation

Our processing consists of taking a video of a vibrating structure and computing the displacement signal everywhere on the structure in the image using a technique related to phase-based motion magnification [9]. Peaks in the Fourier transform of the displacement signal are used to compute the modal frequencies. For each modal frequency, the displacement signal at all points on the structure in the video is filtered with a narrow temporal bandpass filter centered at the modal frequency. The resulting spatially varying temporally filtered displacement signal can be used to estimate the corresponding mode shape.

The displacement signal is only well defined at edges in the video and then only in the direction perpendicular to the edges. This is because the motion of textureless, homogeneous regions is locally ambiguous. Determining the motion at places where it is ambiguous is an open problem in computer vision known as dense optical flow [10, 11]. However, this approach is often inaccurate and for the purposes of modal detection, it is sufficient to know the motion only at the edges of the structure. In the case of the cantilever beam, the entire beam is an edge and the displacement signal can be determined everywhere on it. We use a technique based on local phase and local amplitude in oriented complex spatial bandpass filters to simultaneously compute the displacement signal and edge strength [12,13]. The edge strength can then be used to perform a spatially local weighted average of the displacement signal to improve SNR as in phase-based motion magnification [9].

The local phase and local amplitude are locally analogous quantities to the phase and amplitude of Fourier series coefficients. The phase controls the location of basis function while the amplitude controls its strength. In the case of the Fourier transform, the phase corresponds to global motion. Local phase gives a way to compute local motion. For a video, with image brightness specified by $I(x, y, t)$ at spatial location (x, y) and time t, the local phase and local amplitude in orientation θ at a frame at time t_0 is computed by spatially bandpassing the frame with a complex filter $G_2^\theta + iH_2^\theta$ to get

$$A_\theta(x, y, t_0)e^{i\phi_\theta(x,y,t_0)} = (G_2^\theta + iH_2^\theta) \otimes I(x, y, t_0) \tag{19.1}$$

where $A_\theta(x, y, t_0)$ is the local amplitude and $\phi_\theta(x, y, t_0)$ is the local phase. The filters G_2^θ and H_2^θ are specified in the appendix [14]. To increase SNR and change the scale on which the filters are operating, the video sequence is downsampled four times in each dimension spatially prior to application of the filters.

It has been demonstrated that constant contours of the local phase through time correspond to the displacement signal [12, 13]. Using the notation of Eq. (19.1), this can be expressed as

$$\phi_\theta(x, y, t) = c \tag{19.2}$$

for some constant c. Differentiating with respect to time yields

$$\left(\frac{\partial\phi_\theta(x, y, t)}{\partial x}, \frac{\partial\phi_\theta(x, y, t)}{\partial y}, \frac{\partial\phi_\theta(x, y, t)}{\partial t}\right) \cdot (u, v, 1) = 0 \tag{19.3}$$

where u and v are the velocity in the x and y directions respectively. It is approximately the case that $\frac{\partial\phi_0(x,y,t)}{\partial y} \approx 0$ and $\frac{\partial\phi_{\pi/2}(x,y,t)}{\partial x} \approx 0$. Thus, the velocity in units of pixel is

$$u = -\left(\frac{\partial\phi_0(x, y, t)}{\partial x}\right)^{-1} \frac{\partial\phi_0(x, y, t)}{\partial t} \quad \text{and} \quad v = -\left(\frac{\partial\phi_{\pi/2}(x, y, t)}{\partial y}\right)^{-1} \frac{\partial\phi_{\pi/2}(x, y, t)}{\partial t} \tag{19.4}$$

The velocity between the ith frame and the first frame for all i is computed to give a displacement signal in time. The SNR of this signal is increased by performing a spatially local weighted average of the displacement signal using the local amplitude as weights. The displacement signal is converted to units of millimeters by multiplying by the length of an object in the scene divided by the number of pixels it spans.

The result of the aforementioned processing is a displacement signal at all points in the image. Peaks in the Fourier transform of the resulting signal correspond to modal frequencies. Once the modal frequencies are determined, the spatially varying displacement signal can be temporally filtered around each modal frequency. The user can then specify points along the cantilever beam at which to compute the corresponding mode shape.

19.3 Experimental Setups

19.3.1 Verification Test

In order to validate the camera as a sensor for the measurement of displacements and mode shapes an experiment was formulated to compare the results to standard sensors. An accelerometer was mounted on a cantilever beam, and the motion of the accelerometer was simultaneously measured by a laser vibrometer, an accelerometer, and a high speed camera, as shown in Fig. 19.1a. A screenshot of the video from the camera is shown in Fig. 19.1b, and the resolution of the camera was 480×288, and the frame rate was 5,000 frames per second. In the plane of the accelerometer, the video frame was 104 mm wide. The cantilever beam was excited with an impact hammer, and the subsequent vibration was measured for comparison. The velocity time series from the laser vibrometer was integrated to obtain displacement to verify against the displacements derived from camera measurements of the optical flow of the accelerometer movement. Time synchronization was not possible between the camera and laser vibrometer data set, so in the data the time series were aligned by hand. The data from the laser vibrometer, accelerometer, and camera derived displacement was fast Fourier transformed (FFT), and integrated to be displacement so that the frequency peaks and noise floors could be directly compared.

19.3.2 Cantilever Beam Test

To test the camera as a sensor for determining the mode shape of structures, an experiment measuring a cantilever beam was formulated. The cantilever beam was instrumented with nine accelerometers so that the extracted mode shapes from the accelerometers could be compared with those extracted from the camera data. As before, the beam was excited with an impact hammer and the subsequent vibration was measured by the camera and accelerometers. Figure 19.2a shows a side view of the instrumented cantilever beam, and Fig. 19.2b shows a screenshot from the camera video. Video was taken with the camera at 1,500 frames per second, and the resolution of the video was 1,056×200. In the plane of the column, the video frame was approximately 124 mm wide.

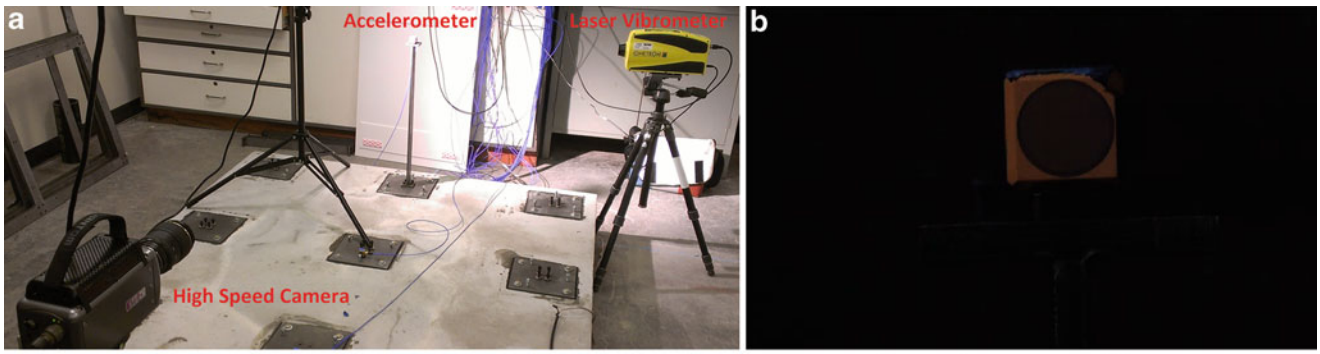

Fig. 19.1 Experimental setup for verification test (**a**) and frame from high speed camera video (**b**)

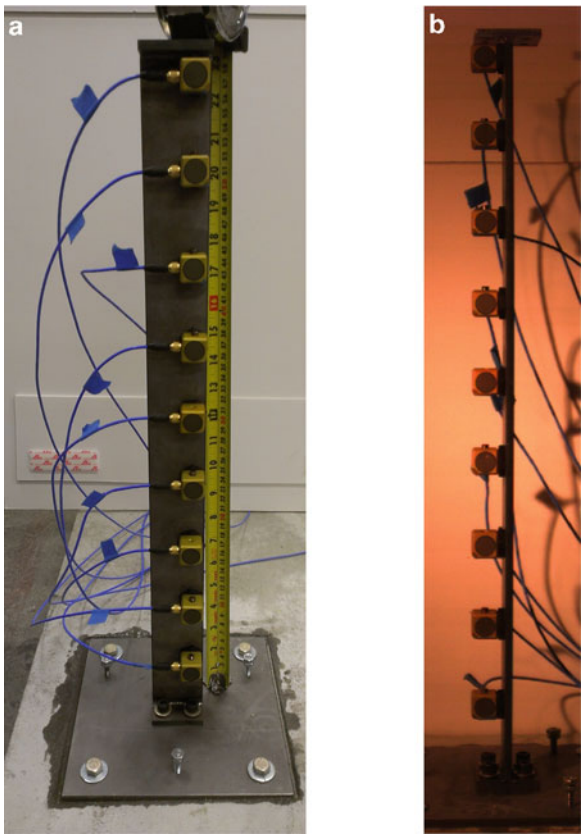

Fig. 19.2 Cantilever beam experimental setup: instrumented cantilever beam side view (**a**), screenshot from video camera (**b**)

19.4 Results

19.4.1 Verification Test

The results of the verification measurement were the various signals of the accelerometer movement as measured by a laser vibrometer, an accelerometer, and a high speed camera. The displacement from the camera was extracted using the local phase of the measured video (Sect. 19.2). The raw signals were the displacement time series from the camera, velocity time series from the laser vibrometer, and acceleration from the accelerometer. To directly compare the time series results, the laser vibrometer velocity time series was integrated numerically and results are shown in Fig. 19.3. The displacement derived from the camera closely matches the integrated laser vibrometer displacement for the whole 9 s of data. In general however, the camera signal shows less detail and is more noisy than the laser vibrometer.

To compare the noise floor of the displacement derived from the camera with the other measurement methods, the signals were fast Fourier transformed and integrated in the frequency domain to obtain the displacements. The plot comparing them is shown in Fig. 19.4. Both the accelerometer and laser vibrometer data show 8 resonant frequencies above the noise floor from 0 to 2,500 Hz, while the camera only shows the first 4 resonant frequencies of the cantilever beam. The noise floor of the camera for this 9 s measurement is approximately 40 nm, while the laser vibrometer has a noise floor of about 0.2 nm, and the accelerometer has a noise floor of about 0.02 nm. Given the conversion factor of 480 pixels for 104 mm, and accounting for the length of the measurement, this gives a noise floor of the camera of approximately 1×10^{-5} pixels per root Hertz. This verification measurement gives us reasonable confidence that the mode shapes of a column can be successfully measured by extracting displacement from video measured with a high speed camera.

19.4.2 Cantilever Beam Test

The method for extracting mode shapes of the cantilever beam is analogous to the method used to extract displacement from the high speed camera video in the verification test. The accelerometer instrumented cantilever beam was measured with the high speed camera and the video was cropped to a region containing only one of each of the nine accelerometers.

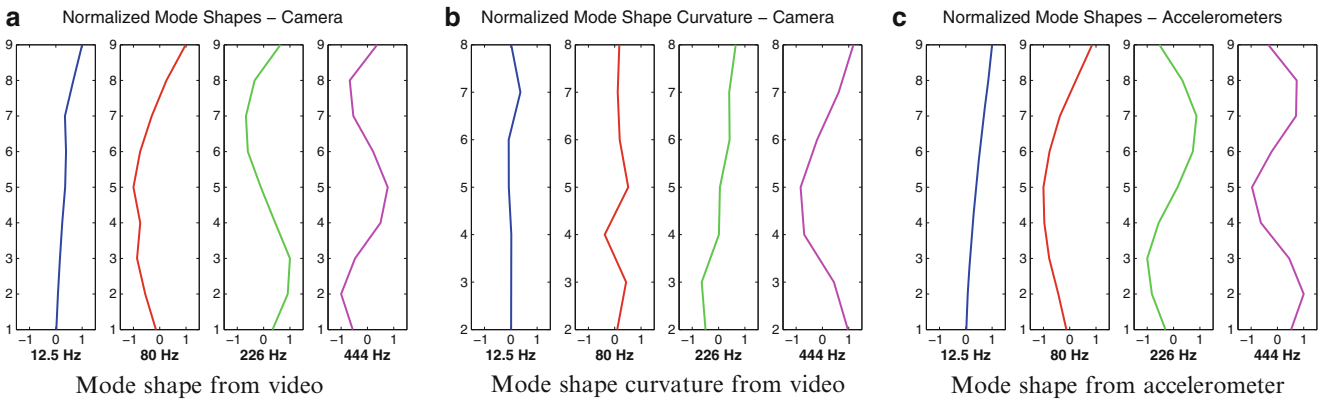

Fig. 19.5 Normalized mode shapes from displacements extracted from camera video (**a**), normalized mode shape curvature from camera video (**b**) and normalized mode shape from accelerometers (**c**)

demonstrating that the data extracted from the camera could be useful for eventual damage detection in structures. It is expected that the camera can be a much easier way of instrumenting a structure with a denser set of measurements which would be useful for more accurate determination of mode shape and mode shape curvature.

The cantilever beam was instrumented with accelerometers to provide mode shapes from a conventional method of measurement for comparison. The mode shapes from the accelerometer data are shown in Fig. 19.5c. The camera extracted mode shapes compare well to mode shapes derived from the accelerometer data.

19.5 Conclusion

In this paper we have assessed motion magnification for extracting displacements from high speed video and demonstrated the algorithm's capability of extracting the mode shapes of a cantilever beam from a video measurement. Motion magnification represents a novel method for deriving mode shapes and displacements from videos of vibrating structures. Changes in local phase in the video are processed to determine the displacement signal at every point in the video. When the displacement signal of an accelerometer on a beam is computed, the displacements extracted closely match those extracted by a laser vibrometer, and the resulting noise floor of the camera is approximately 1×10^{-5} pixels per root Hertz. The first four mode shapes of an instrumented cantilever beam at 12.5, 80, 226, and 444 Hz were extracted and compared favorably to both the expected theoretical mode shapes and the accelerometer data derived mode shapes. Mode shape curvature was calculated from the video extracted mode shapes as a basis for the potential use of the technique for damage detection.

Several areas of this methodology can be improved with further research. Automation of the algorithms used such that moving objects in the frame of the video can have their mode shapes extracted would be immensely useful for modal analysis. For the measurement of outdoor structures, further challenges need to be overcome, specifically atmospheric aberration due to changes in the index of refraction of air with variations in temperature. This issue may be solved by further use of the methods derived from motion magnification. Further studies on using the camera derived displacements for damage detection in structures will also be conducted. The eventual goal is to be able to measure any structure, measure the displacement, characterize it's modal behavior, and potentially detect any damage.

Acknowledgements The authors acknowledge the support provided by Royal Dutch Shell through the MIT Energy Initiative, and thank chief scientists Dr. Dirk Smit, Dr. Sergio Kapusta, project manager Dr. Yile Li, and Shell-MIT liaison Dr. Jonathan Kane for their oversight of this work. We also acknowledge Draper Laboratory for providing experimental equipment. At the time of this work, Neal Wadhwa was supported by the DoD through the NDSEG fellowship program. Special thanks are due to Reza Mohammadi for his help with experimental collection of the data, specifically as the hammer man.

Table 19.1 Filter coefficients to compute horizontal and vertical local phase and local amplitude

Tap #	G_{f1}	G_{f2}	H_{f1}	H_{f2}
−4	0.0094	0.0008	−0.0098	0.0008
−3	0.1148	0.0176	−0.0618	0.0176
−2	0.3964	0.1660	0.0998	0.1660
−1	−0.0601	0.6383	0.7551	0.6383
0	−0.9213	1.0000	0.0000	1.0000
1	−0.0601	0.6383	−0.7551	0.6383
2	0.3964	0.1660	−0.0998	0.1660
3	0.1148	0.0480	0.0618	0.0176
4	0.0094	0.0008	0.0098	0.0008

Filter	Filter in x	Filter in y
Real horizontal (G_2^0)	G_{f1}	G_{f2}
Imaginary horizontal (H_2^0)	H_{f1}	H_{f2}
Real vertical ($G_2^{\pi/2}$)	G_{f2}	G_{f1}
Imaginary vertical ($H_2^{\pi/2}$)	H_{f2}	H_{f1}

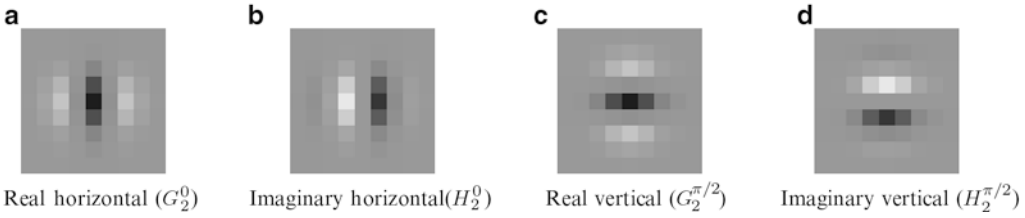

Fig. 19.6 Two dimensional representation of filters used to compute horizontal (**a**-**b**) and vertical (**c**-**d**) local phase and local amplitude

Appendix: Steerable Filter Taps

Freeman et al. [14] specify steerable filters that we use in this paper. For convenience, we reproduce their filters here in Table 19.1 and Fig. 19.6.

References

1. Farrar CR, Darling TW, Migliori A, Baker WE (1999) Microwave interferometers for non-contact vibration measurements on large structures. Mech Syst Signal Process 13(2):241–253
2. Stanbridge A, Ewins D, Khan A (2000) Modal testing using impact excitation and a scanning LDV. Shock Vib 7(2):91–100
3. Patsias S, Staszewskiy W (2002) Damage detection using optical measurements and wavelets. Struct Health Monit 1(1):5–22
4. Wahbeh AM, Caffrey JP, Masri SF (2003) A vision-based approach for the direct measurement of displacements in vibrating systems. Smart Mater Struct 12(5):785
5. Lee JJ, Shinozuka M (2006) A vision-based system for remote sensing of bridge displacement. Ndt & E Int 39(5):425–431
6. Caetano E, Silva S, Bateira J (2011) A vision system for vibration monitoring of civil engineering structures. Exp Tech 35(4):74–82
7. Liu C, Torralba A, Freeman WT, Durand F, Adelson EH (2005) Motion magnification. ACM Trans Graph 24:519–526
8. Wu H-Y, Rubinstein M, Shih E, Guttag J, Durand F, Freeman W (2012) Eulerian video magnification for revealing subtle changes in the world. ACM Trans Graph (Proc SIGGRAPH 2012) 31(4):65
9. Wadhwa N, Rubinstein M, Durand F, Freeman WT (2013) Phase-based video motion processing. ACM Trans Graph (Proc SIGGRAPH 2013) 32(4):80
10. Horn B, Schunck B (1981) Determining optical flow. Artif Intell 17(1–3):185–203
11. Lucas BD, Kanade T (1981) An iterative image registration technique with an application to stereo vision. In: Proceedings of the 7th international joint conference on artificial intelligence (IJCAI '81), pp 674–679, Apr 1981
12. Fleet DJ, Jepson AD (1990) Computation of component image velocity from local phase information. Int J Comput Vis 5(1)77–104
13. Gautama T, Van Hulle M (2002) A phase-based approach to the estimation of the optical flow field using spatial filtering. IEEE Trans Neural Network 13(5):1127–1136
14. Freeman WT, Adelson EH (1991) The design and use of steerable filters. IEEE Trans Pattern Anal Mach Intell 13(9):891–906